research articles Journal of proteome research

NMR Metabolic Profiling of *Aspergillus nidulans* to Monitor Drug and Protein Activity

Paxton Forgue,[†] Steven Halouska,[†] Mark Werth,[§] Kaimei Xu,[‡] Steve Harris,[‡] and Robert Powers*,[†]

Departments of Chemistry and Plant Pathology, University of Nebraska-Lincoln, Lincoln, Nebraska 68588 and Department of Chemistry, Nebraska Wesleyan University, Lincoln, Nebraska 68504

Received March 23, 2006

We describe a general protocol for using comparative NMR metabolomics data to infer in vivo efficacy, specificity and toxicity of chemical leads within a drug discovery program. The methodology is demonstrated using *Aspergillus nidulans* to monitor the activity of urate oxidase and orotidine-5′-phosphate decarboxylase and the impact of 8-azaxanthine, an inhibitor of urate oxidase. 8-azaxanthine is shown to inhibit *A. nidulans* hyphal growth by in vivo inactivation of urate oxidase.

Keywords: drug discovery • NMR • metabolomics • principle component analysis • *Aspergillus nidulans* • purine degradation pathway • pyrimidine biosynthetic pathway

Introduction

Demands for drug discovery have increased dramatically over the years, due to the continual identification of new protein targets associated with various diseases.[1] New technology and strategies have been used to reduce these demands to help speed up the process of developing new and safer drugs.[2] Due to the inherent complexity of drug discovery, the success rate of identifying new therapeutics is very low while the corresponding cost of research and clinical trials is ~$800 million dollars per marketed drug.[3−5] There has been a decline in the productivity of drug discovery efforts despite a 13% annual growth rate in research budgets.[6] Estimates indicate that only one new chemical entity (NCE) out of 25 NCEs identified from active research projects will become a marketable drug. The current success rate of clinical trials is only 11%.[7,8] Issues related to pharmacokinetics, toxicity, efficacy and cost are major factors that negatively impact drug discovery and development programs.[9−11] A significant amount of the associated cost is encountered in the clinic, therefore; strategies are being implemented to assess the "developability" of chemical leads at early stages of drug discovery from available in vitro data to prioritize chemical leads for further development.[12] Additionally, the application of systems biology to drug discovery presents a potentially powerful tool to identify and avoid toxicity and efficacy problems prior to initiating clinical trials.[13,14]

In this context, a disease state reflects the perturbation in the operation of a network at the cellular or organism level. The comparison of these healthy and diseased networks identifies critical intersection points that are associated with disease markers and drug activity. One means of analyzing the state of a biological system is achieved by monitoring the metabolome.[15−17] The function and activity of numerous proteins encoded by the genome are directly or indirectly associated with the relative concentration of cellular metabolites,[18] which is the underlying concept of chemical genomics.[19] Thus, measuring changes in metabolite concentrations provides direct information on changes in the cellular activity of proteins.

Both NMR[20,21] and mass spectroscopy[22,23] are being used to detect these perturbations. NMR is routinely being applied to monitor drug toxicity or identify disease markers by following changes in metabolite concentrations in biofluids.[20,24−30] This is routinely achieved by simply collecting one-dimensional ^{1}H NMR spectra of the biofluid. The resulting NMR spectrum tends to be extremely complex due to the presence of hundreds of low molecular-weight compounds where visual inspection to identify metabolite concentration changes is relatively cumbersome and impractical for large data sets. Instead, principal component analysis (PCA) is used to decipher changes in a series of NMR spectra caused by changes in metabolite concentrations.[31,32] PCA is a well established statistical technique that determines the directions of largest variations in the NMR data set. The PCA data is typically presented as a two-dimensional plot (scores plot) where the coordinate axis corresponds to the principal components representing the directions of the two largest variations in the NMR data set (PC1, PC2). PCA results in a reduction of the multivariable NMR spectra into a simpler coordinate system of PCs, where each NMR spectra is reduced to a single point in the PC coordinate axis. Similar NMR spectra will cluster together in PC coordinate space and variations along any of the PC axis will highlight experimental differences in the spectra.

Metabolomics has a range of potential roles in drug discovery that includes target identification, chemical lead optimization,

* To whom correspondence should be addressed: Department of Chemistry, 722 Hamilton Hall, University of Nebraska, Lincoln, Nebraska 68588. Tel: (402) 472-3039. Fax (402) 472-9402. E-mail: rpowers3@unl.edu.
[†] Department of Chemistry, University of Nebraska-Lincoln.
[‡] Department of Plant Pathology, University of Nebraska-Lincoln.
[§] Department of Chemistry, Nebraska Wesleyan University.

10.1021/pr060114v CCC: $33.50
Published on Web 07/08/2006

and toxicity and efficacy studies, where the metabolomic strategy is extremely time efficient and cost-effective compared to clinical trials.[18,21,33] In addition to biofluids, metablome samples from cell lysis have been used to identify silent mutations[34] and classify clinical bacterial strains.[35] In this paper, we describe the application of NMR and principal component analysis (PCA)[31,32] to monitor the metabolome of the filamentous fungus *Aspergillus nidulans*,[36,37] as a model system to develop new antifungals.[38] Specifically, we demonstrate a general protocol that uses NMR metabolomics to follow the in vivo activity of a drug discovery protein target after treating cells with a chemical lead. In this manner, the in vivo activity and potential toxic side-effects of these drugs can be ascertained prior to initiating expensive animal and human studies. We followed the activity of urate oxidase (E.C. 1.7.3.3), an enzyme that catalyzes the conversion of uric acid to allantoin in the purine degradation pathway, and orotidine-5′-phosphate decarboxylase (E.C. 4.1.1.23), an enzyme in the pyrimidine biosynthetic pathway that catalyzes the conversion of orotidine 5′-phosphate to uridine 5′-phosphate, in response to inhibitor activity and mutagenesis.

Materials and Methods

Microscopy. *A* 2-μL portion of conidiospores were added to 10 mL of YGV media (2% dextrose, 0.5% yeast extract, and vitamins), which was then poured into 60 mm Petri dishes containing two coverslips.[39] The spores were allowed to germinate at 30.0 °C for 12 h. Growing hyphae were then stained with FITC-conjugated wheat germ agglutinin (i.e., lectin) for 5 min to label cell wall chitin. The drug treated cells were transferred to fresh YGV containing 5 mM of 8-azaxanthine (AZA), a known inhibitor of urate oxidase,[40,41] and incubated at 30.0 °C for two more hours. Coverslips were then transferred to a fixing solution for 15 min, washed in double distilled water for 5 min and mounted on glass slides.[39] Microscopy results were obtained using a BX51 fluorescent microscope (Olympus, Melville, NY). Images were captured with a Photometrics CoolSnap HQ CCD camera (Roper Scientific, Duluth, GA) and processed using IPLab software (Scanalytics Inc. Rockville, MD) and Adobe PhotoShop 6.0 (Adobe Systems Inc., San Jose, CA).

Preparation of NMR Metabolomic Samples. Obtaining reliable results is critically dependent on the consistency of sample handling, data collection, and processing so any variability reflects changes in the state of the metabolome not in the variability of data collection. The approach requires collecting multiple data points to identify clear data clusters that differentiate the different spore types. A total of 50 *Aspergillus nidulans* samples were grown and obtained for NMR metabolomics experiments. Ten repeat *A. nidulans* samples were grown for the following five groups: (1) wild-type *A. nidulans*, (2) wild type *A. nidulans* with 5 mM AZA, (3) *A. nidulans uaZ14* mutant coding for urate oxidase[42], (4) *A. nidulans uaZ14* mutant with 5 mM AZA, and (5) *A. nidulans pyrG89* mutant coding for orotidine-5′-phosphate decarboxylase[43]. One-hundred microliters of spores were added to 10 mL of complete media supplemented with inositol and ammonium nitrate added for the *uaZ14* mutant, or 10 mM uracil and 5 mM uridine for the *pyrG89* mutant. Spores were incubated in 250 mL flasks at 30.0 °C at 200 rpm for 16 h. After 16 h, 100 μL of 100 mg/mL AZA in DMSO was added to the selected cultures, and growth continued for an additional 2 h before harvesting. For the *pyrG89* mutant, cultures were transferred to unsupplemented complete media after 16 h growth.

Fungal mycelia were vacuum filtered and washed with 50 mM potassium phosphate buffer. They were immediately frozen in liquid nitrogen after filtration, and then ground using a mortar and pestle. Ground mycelia were stored in eppendorf tubes on ice until later use. A 1-mL portion of 99.8% D_2O solution containing 50 mM potassium phosphate buffer at pH of 7.2, and 50 μM TMSP was added to the ground cells which were then stirred and centrifuged. A 500-μL portion of spore free extract was transferred to an NMR tube.

NMR Data Collection, Processing, and Statistical Analysis. The NMR spectra were collected on a Bruker 500 MHz Avance spectrometer equipped with a triple-resonance, *Z*-axis gradient cryoprobe. A BACS-120 sample changer with Bruker Icon software was used to automate the NMR data collection. ^{1}H NMR spectra were collected with solvent presaturation, a sweep-width of 5482.5 Hz, 32K data points at 298 K. A total of 4 dummy scans and 256 scans were used to obtain the NMR spectra.

The 5 groups of 10 NMR spectra were processed automatically using a standard processing macro in the ACD/1D NMR manager version 8.0 (Advanced Chemistry Development, Inc., Toronto, Ontario). The residual H_2O NMR resonance between 4.52 and 5.45 ppm was set to 0 and excluded from bucketing and PCA analysis. All spectra were phased, baseline corrected, and the TMSP peak was set to 0.0 ppm. The baseline was corrected using spectrum averaging. The spectrum regions that do not contain signals are defined by using a rectangular box (box half-width of 30 points). A noise factor of 5 was used to differentiate between real peaks and noise regions. The baseline is constructed by averaging the spectrum curve over these regions. Intelligent bucketing was used to integrate each region with a bin size of 0.025 ppm with a width looseness of 50%. Intelligent bucketing option in the ACD software chooses integral divisions based on local minima and will avoid common spectral variations due to minor pH or salt differences. The table of integral was transferred to MS Excel, which was used to arrange all 50 samples based on the five groups described above. An Excel macro was then used to combine the NMR spectra into a single file to normalize the binned intensities to a total integrated intensity of 1.0. The table was then imported into SIMCA (UMETRICS, Kinnelon, NJ) for PCA analysis using the programs standard parameters. Our previous analysis indicated that the presence of noise regions in the bucketing of NMR spectra can result in large and irrelevant variations in the PCA clustering.[44] Exclusion of the noise regions of the ^{1}H NMR spectra was accomplished by an Excel macro that set the value of every bin below a certain intensity threshold to zero. Two sets of PCA data were generated corresponding to the following: (1) *A. nidulans* wild-type, *A. nidulans* wild-type with AZA, *A. nidulans uaZ14* mutant, and *A. nidulans uaZ14* mutant with AZA; (2) *A. nidulans* wild-type, *A. nidulans uaZ14* mutant, and *A. nidulans pyrG89* mutant.

Results and Discussion

***Aspergillus nidulans* Metabolome Model System.** *A. nidulans* is a commonly used model organism for filamentous fungus because of its close relatedness to both pathogenic and industrially important fungi.[37] Despite the common use of *A. nidulans* as a model organism, there is only one prior metabolomic study that utilized *A. nidulans*.[45] Nevertheless, it is widely recognized that fungal metabolomic analysis is extremely valuable for functional genomics.[46,47] Over 2000 *A. nidulans* mutants are publicly available,[39,48,49] including the *uaZ14*[42] and *pyrG89*[43] mutants. The *A. nidulans uaZ* gene encodes for urate

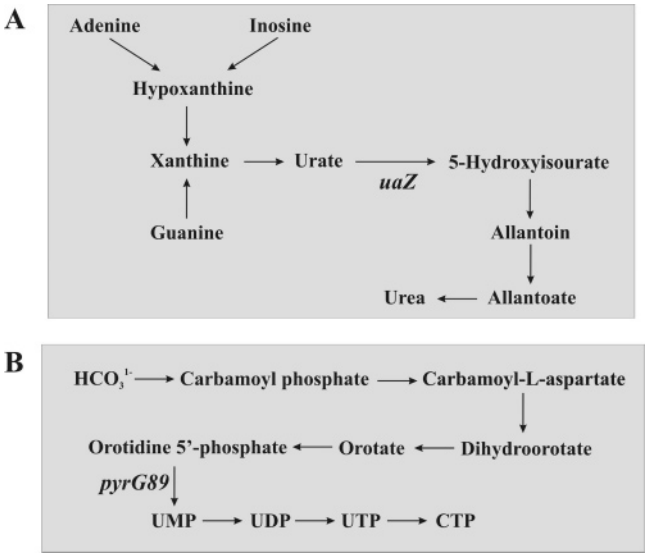

Figure 1. (a) *uaZ14* mutant in *A. nidulans* disrupts the oxidation of urate in the purine degradation pathway. (b) *pyrG89* mutant in *A. nidulans* disrupts the conversion of orotidine 5′-phosphate to uridine 5′-phosphate as part of the pyrimidine biosynthetic pathway.

oxidase(Uox),[50,51] an enzyme that converts uric acid to allantoin as part of the purine degradation pathway[52] (Figure 1A). The *A. nidulans uaZ14* mutant eliminates the normal function of urate oxidase. The *uaZ14* mutation is caused by a single base substitution that generates a nonsense allele. There is no cross-reactive Uox protein present in the cell when this mutant was probed with a specific antibody.[53] Thus, the mutant is a true null allele.

The *uaZ14* mutant also inhibits *A. nidulans* growth. This is evident by the activity of 8-azaxanthine (AZA), a known inhibitor of urate oxidase.[40,41] AZA inhibits the growth of *A. nidulans* and depresses the urate oxidase activity as observed by changes in uric acid concentration. Similarly, the structure of urate oxidase from *Aspergillus flavus* has been determined by X-ray crystallography that clearly shows 8-azaxanthine binding in the enzymes active-site.[54,55]

The *A. nidulans pyrG89* gene encodes for orotidine-5′-phosphate decarboxylase (OMP),[56,57] an enzyme that converts orotidine 5′-phosphate to uridine 5′-phosphate as part of the pyrimidine biosynthetic pathway[58,59] (Figure 1B). OMP is the most proficient enzyme known and catalyzes this difficult conversion without the aid of metals, cofactors or other small molecules. OMP is an exhaustively studied metabolic enzyme that includes numerous X-ray structures.[60] Since pyrimidines are generally important for a variety of cell function and highly regulated,[61−64] inhibition of the pyrimidine biosynthetic pathway tends to stimulate or up-regulate pyrimidine salvage pathways.[65,66] Thus, pyrimidine biosynthetic pathways are a common target for drug discovery.[66−68] The *A. nidulans pyrG89* mutant eliminates the normal function of OMP and is similar to *uaZ14*, where both are recessive, loss-of-function mutations. The *pyrG89*mutant has not been characterized at the DNA or the protein level. But, the growth phenotype of a *pyrG* deletion mutant is indistinguishable from the *pyrG89* mutant suggesting *pyrG89* is also a null allele.

A. nidulans uaZ14[42] and *pyrG89*[43] mutants present a unique model system to explore the potential utility of NMR-based metabolomics to monitor in vivo drug activity. To test this

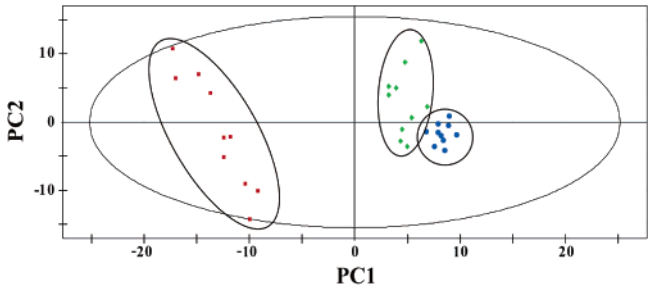

Figure 2. PCA scoring plot for the comparison of *A. nidulans* A28 (wild-type) (green ♦), Mad293 (*uaZ14*) (blue ●), and AML8 (*pyrG89*) (red ■).

hypothesis, we first verified that perturbations in the *A. nidulans* metabolome resulting from the *uaZ14* and *pyrG89* mutants were unique enough to be monitored by NMR and that these metabolome differences could be differentiated by PCA analysis. Effectively, can the PCA analysis of the NMR metabolomics data distinguish the mutants from each other and from wild-type mycelia? Second, we demonstrate that the activity and cellular target of a known drug (AZA) can be followed by monitoring its impact on the *A. nidulans* metabolome.

Monitoring Protein Activity Using NMR Metabolomics. Purines and pyrimidines are major synthetic components of cofactors, proteins, RNA and DNA and thus are essential for cell viability as evident by the presence of biosynthetic, salvage, and degradation pathways.[52,58] Purines and pyrimidines are chemically unique, which results in unique collections of substrates and products in the various metabolic pathways that involve these compounds. This is clearly evident by the metabolites found in the pyrimidine biosynthetic and purine degradation pathways listed in Figure 1. Thus, even though purines and pyrimidines are clearly related in their biochemical roles within a cell, these collections of metabolites present unique markers to follow the individual activity of purine and pyrimidine pathways and the activity of their associated proteins. The *differential* comparison of metabolomes would identify these major changes in metabolite concentrations, which in turn would highlight activity changes in the purine and pyrimidine pathways. In this manner, the metabolome for *A. nidulans* mutants *uaZ14* and *pyrG89* are expected to be different from each other and different from wild-type spores. Similar results have been seen for *Saccharomyces cerevisiae* and *Bacillus cereus*.[34,35]

NMR provides a simple approach for measuring metabolomic data with minimal sample handling.[31,32] Small volumes of *A. nidulans* mycelia (10 mL) were harvested by rapidly freezing in liquid nitrogen followed by grinding in a mortar and pestle. The biomass was suspended in a deuterated buffer, centrifuged, and simply transferred into an NMR tube. A one-dimensional ^{1}H NMR spectrum was then collected on the samples to provide a "fingerprint" of the metabolites present in the fungus. Principal component analysis (PCA)[31,32] was used to compare the NMR metabolomic data to identify major differences between the spectra. Ten replicates each of *A. nidulans* strains A28 (wild type), Mad293 (*uaZ14*), and AML8 (*pyrG89*) were grown and their metabolome analyzed by NMR and PCA. Figure 2 illustrates the resulting PCA scores plot, which identifies the largest differences between the NMR spectra based on relative displacements along the PC1 and PC2 axis. It is clearly evident that the three *A. nidulans* strains form three distinct clusters in the PCA scores plot highlighting the relative differences in their metabolome composition. The proportional clustering in the PCA scores plot also suggests the relative sim-

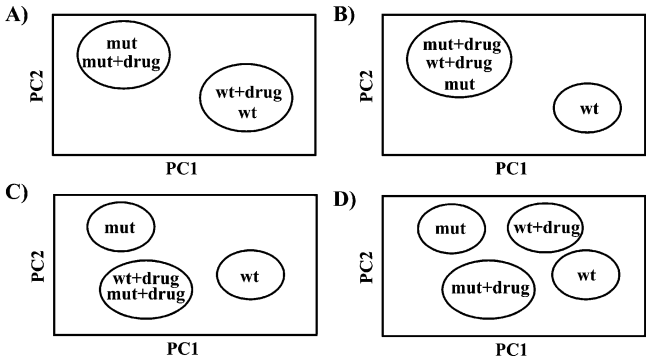

Figure 3. Cartoon illustrations of hypothetical PCA scores plot for the following scenarios (a) inactive compound, (b) active and selective inhibitor, (c) active, nonselective inhibition of target and secondary protein, and (d) active, nonselective preferential inhibition of secondary protein. Labels correspond to: wild-type cells (wt) and mutant cells (mut).

ilarity between the different metabolomes. The *pyrG89* mutant is clustered farther away from the wild type and *uaZ14* mutant because the *pyrG89* mutation affects both the pyrimidine biosynthetic and salvage pathways.[65,66] Therefore, it is not surprising that a larger change in this metabolome was observed.

Since the NMR metabolomic data presented here clearly differentiates *uaZ14* and *pyrG89* mutants while also distinguishing the mutants from wild-type mycelia, the approach should equally be applicable to monitoring the activity of a drug targeting these proteins. Effectively, the *uaZ14* and *pyrG89* mutants represent the extreme condition of a highly active compound that completely and irreversibly inhibits these enzymes.

Model for in Vivo Drug Activity from NMR Metabolomics Data. NMR metabolomic studies of in vivo drug activity may provide an approach to obtain initial data on efficacy, selectivity and toxicity for chemical leads. Our approach simply requires comparing the metabolome between wild-type and mutant cells, where the drug discovery target is inactivated or diminished in activity in the mutant cell line. Both the wild-type and mutant cells are also treated with the chemical lead, which is a potential inhibitor of the protein target. PCA of the resulting NMR metabolomic data has three potential outcomes directly related to the activity and selectivity of the chemical lead.

In the absence of treatment with an inhibitor, the mutant and wild-type cells should cluster distinctly in the PCA scores plot due to the inactivation of the protein target in the mutant cells. If the compound is completely inactive in vivo, then the wild-type cells in the presence and absence of the compound would cluster together, but still separate from the mutant cells (Figure 3A). Conversely, if the compound is active and selective, then the wild-type cells in the presence of the compound would cluster together with the mutant cells in the presence and absence of the chemical lead (Figure 3B). This is because the target protein is now inactivated in all three cell growths due to either the protein mutation or the activity of the inhibitor. There are two potential variations in the PCA scores clustering if the compound is active and nonselective.

If the compound similarly inactivates both the desired protein target and secondary target(s), then both the wild-type and mutant cells in the presence of the compound will form a cluster distinct from the wild-type and mutant cells in the absence of the compound (Figure 3C). The wild-type and mutant cells in the presence of the inhibitor would experience a similar change in the metabolome due to the inactivation of *all* the affected proteins through either the activity of the inhibitor and/or by the genetic mutation. The observed secondary activity for the chemical lead may potentially contribute to toxic side-effects.[69,70] This information may be used to eliminate the compound from further development or as a tool to monitor the effectiveness of chemical modifications to eliminate this undesirable secondary activity.

If the compound is preferentially inhibiting a secondary protein, then four distinct clusters would be observed (Figure 3D). Only the mutant in the presence of the compound would have both the protein target and the secondary target(s) inactivated. Both the mutant cells without the drug and the wild-type cells with the drug would have different proteins inactivated, the protein target and secondary target(s), respectively. A compound that exhibits this type of metabolic profile would invariably be of minimal value as a chemical lead in a drug discovery program and would probably be eliminated from further development.

The idealized scenarios described above assume that inactivating a protein through genetic mutation and the reversible binding of an inhibitor will have essentially the same impact on the metabolome. There may be some situations where this may not occur. The presence of *some* misfolded or aggregated proteins may affect the physiology of the cell and correspondingly change the metabolome distinctly from a chemically inhibited protein.[71] Nevertheless, the majority of defective proteins are targeted for storage and cellular degradation.[72−74] Defective proteins are common and account for 30% of synthesized proteins.[74] This implies that, in general, a genetically mutated protein may not significantly alter the metabolome since the simple presence of the defective protein may not induce any cellular processes that are not normally active. Also, depending on the severity of the mutation, the cellular response to a defective protein may primarily focus on producing a functional protein and delay the degradation process.[72]

Multifunctional proteins and proteins involved in multiple signaling pathways may also present challenges in properly analyzing metabolomic data. The complete elimination of a multifunctional protein through mutation would obviously affect all the biological pathways associated with this protein with the corresponding impact on the metabolome. But, an inhibitor may only be designed to selectively inhibit one of the protein's functions, where the remainder of its activities would remain intact. This would result in a consistent difference between the metabolomes of the mutant cells and drug treated wild-type cells despite the correct and desired inhibitor activity.

The judicious choice of the genetic mutations may effectively minimize or eliminate these potential problems. As an example, identifying a point mutation that effectively knocks out the activity of one function of a multifunctional protein without misfolding or aggregating the protein would be an optimal goal. This also implies that a well-characterized protein will aid in the design of precise deletions and point mutations and inevitably benefit the application of metabolomic data to analyze in vivo drug activity and specificity. While the ability to generate a mutant cell line for a *specific* protein target is unknown and may pose a particular challenge, numerous mutant cell lines have been successfully developed. Almost 12 000 viable deletion mutants are or will soon be available for yeast and filamentous fungi alone.[49,75,76] Of course, a lethal gene deletion is problematic and limits the utility of metabolomic data. RNA interference may be used to generate partial loss of protein activity and mimic the effect of a chemical

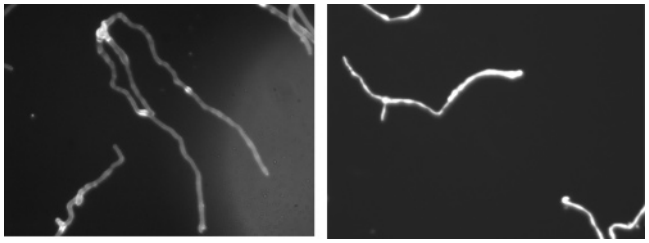

Figure 4. Comparison of the untreated *A. nidulans* fungus (left) vs the fungus treated with 8-azaxanthine (right). Lectin stain, which binds to growing chitin cell walls, indicates the amount of hyphal growth that occurred after the stain. The lack of additional hyphal growth in the presence of AZA is clearly evident by the complete staining of the spores in the right panel.

lead.[77,78] Alternatively, lethal mutations may be rescued using supplemented growth media or chemical rescue.[79] This is illustrated by *pyrG89* and *uaZ14*, which both required supplemented media for growth. It may also be feasible to develop a precise point mutation that only diminishes or increases the activity of the essential protein.[80] Again, the general goal is to identify a change in the metabolome that is correlated with the activity of the protein of interest.

Monitoring in Vivo Drug Activity from NMR Metabolomics Data. The application of NMR metabolomics to monitor the in vivo activity of a drug was tested using a known and predictable system. *A. nidulans uaZ14* mutant mycelium, where urate oxidase is inactive, was compared to a wild-type strain using 8-azaxanthine (AZA), a well-known inhibitor of urate oxidase. First, the in vivo activity of AZA was visually verified by the observation of the drugs ability to inhibit new hyphal growth in *A. nidulans* (Figure 4). *A. nidulans* strain Mad293 was grown for 16 h and then treated with lectin to stain the growing cell walls. One culture was subsequently allowed to continue growth as before, whereas a second was treated with AZA.

The *A. nidulans* growth under steady growth conditions, without nutrient limitations and an air interface, results in a persistent vegetative state with the growth of hyphae and no reproductive structures.[81] Under these conditions, chitin deposition occurs over the entire hyphal surface, though it is most prominent at the immediate hyphal tip. Accordingly, when stained with the FITC-conjugated lectin wheat germ agglutinin, which detects chitin, a band of bright fluorescence is observed at the tip. If hyphae are then returned to lectin-free media, then the former tip remains bright, but new growth from the tip is not stained. When hyphal growth is blocked, as when AZA is added, lectin staining remains intense at the tips due to the absence of new growth. The degradation of hypoxanthine and xanthine to uric acid is an aerobic step in which oxidation occurs. When hyphae are exposed to air, which is essential for the aerobic degradation step, reproductive structures are formed.[82] High concentrations of xanthine and uric acid inhibit the growth of hyphae since the product of the aerobic step is abundant.

The PCA scores plot of *A. nidulans uaZ14* mutant and wild-type spores in the presence and absence of AZA is shown in Figure 5. As expected the *A. nidulans* wild-type spores in the absence of AZA forms a separate and distinct cluster. *A. nidulans uaZ14* mutant spores in the presence and absence of AZA and the *A.* nidulans wild-type spores in the presence of AZA all cluster close together in the PCA scores plot. Again, this is consistent with the specific inhibition of urate oxidase by AZA as explained in detail above. The observation that there

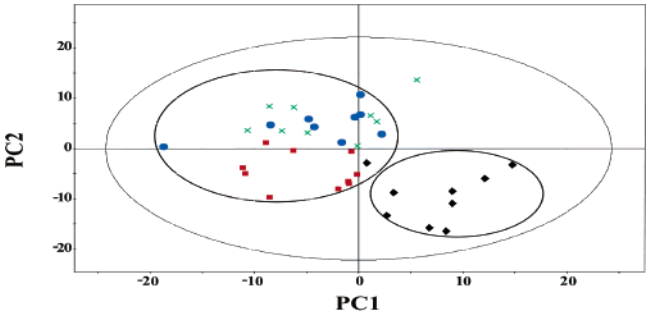

Figure 5. PCA scores plot comparing *A. nidulans uaZ14* mutant (green x), wild-type with AZA (red ■), *uaZ14* mutant with AZA (blue ●), and wild-type cells (♦).

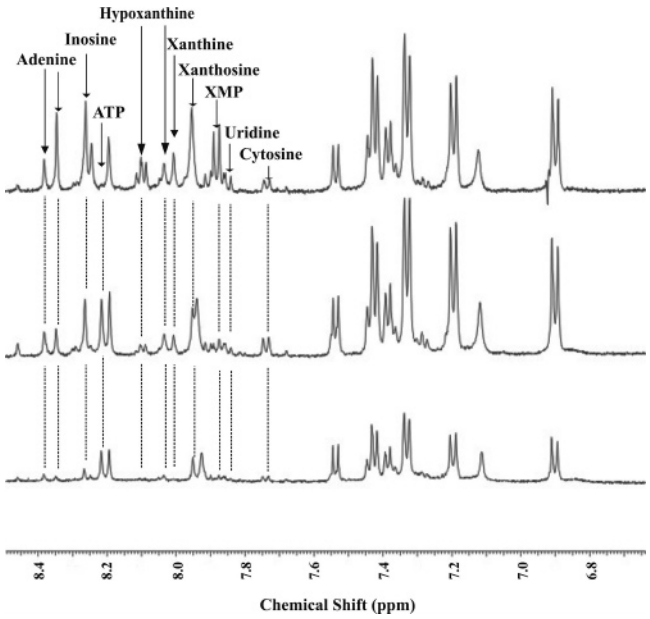

Figure 6. Aromatic regions of NMR spectra in order from top to bottom are: *uaZ14* mutant, wild-type with drug, and wild-type untreated. Arrows identify the adenine, hypoxanthine, inosine and xanthine peaks which are absent or significantly decreased in AZA untreated wild-type mycelia. The peaks are all normalized to the most intense peak in the spectra.

is still some small separation between *A. nidulans* wild-type spores in the presence of AZA and the *A. nidulans uaZ14* mutant spores probably results from residual Uox activity. In the *uaZ14* mutant, Uox activity is completely eliminated, but this is probably not the case for the wild-type spores in the presence of AZA. Since AZA is a reversible inhibitor, a certain fraction of Uox will remain inhibitor-free and can still convert uric acid to allantoin.

Verification that the PCA scores plot clustering is responding to relevant biochemical changes in the metabolome as a result of the inhibition of urate oxidase by AZA is also apparent by comparing NMR spectra. Comparison of the NMR spectra between *A. nidulans* wild-type mycelia and *uaZ14* mutant mycelia in the absence of AZA with *A. nidulans* wild-type mycelia treated with AZA is shown in Figure 6. While the NMR spectra are generally similar, definite variations are seen. The aromatic regions of the *A. nidulans uaZ14* mutant and the AZA treated wild-type mycelia exhibit a higher similarity than wild-type in the absence of AZA. Some metabolites in the purine degradation pathway are invisible by ^{1}H NMR because of the free exchange of the amine hydrogens with the deuterated

solvent and the overall lack of hydrogens in the chemical structure. The NMR peaks at 8.00, 8.10, 8.23, and 8.32 ppm are the most noticeable differences between the *A. nidulans* wild-type NMR spectrum in the absence of AZA compared to the *A. nidulans uaZ14* mutant and the AZA treated wild-type mycelia. These NMR peak are consistent with the purine rings of adenine, hypoxanthine, inosine, and xanthine, which are precursors to urate in the purine degradation pathway (Figure 1). This indicates that the concentration of these metabolites has significantly increased in the *A. nidulans uaZ14* mutant and the AZA treated wild-type mycelia. Again, this is the expected result if AZA selectively inhibits urate oxidase and adenine, inosine, hypoxanthine, and xanthine are not fully metabolized to urea in the purine degradation pathway. The bins corresponding to the NMR peaks for these metabolites were a major contributor to the negative shift in the PCA loadings along PC1 in the PCA scores plot. So as expected, the PCA clustering is primarily based on changes in adenine, inosine, hypoxanthine, and xanthine concentrations, which are due to the change in activity of urate oxidase. In effect, comparison of the PCA loadings with the NMR spectra aids in identifying NMR peaks that incurred the largest difference due to the addition of AZA (please see Supporting Information).

Additional metabolites not directly involved in the purine degradation pathway were also affected by the addition of AZA and the inhibition of Uox. The xanthine salvage and pyrimidine synthesis pathways have metabolites in common with the purine degradation pathway. Because of an increase in xanthine, the xanthine salvage pathway converts some xanthine to xanthosine, and xanthosine-5′-monophosphate (XMP). The conversion of 5-phosphoribosyl 1-pyrophosphate to 5-phosphoribosyl glycineamide is the rate-limiting step in the purine synthesis and purine degradation pathways. A high concentration of xanthine and the inhibition of Uox enable the pyrimidine synthesis pathway to use 5-phosphoribosyl 1-pryophospate. This is evident by the increase in the concentration of uridine and cytosine. These secondary metabolites affected by the inhibition of Uox are also labeled in Figure 6.

The *A. nidulans uaZ14* mutant mycelia in the presence of AZA also provide a negative control for the metabolomic analysis. Adding AZA to the *A. nidulans uaZ14* mutant mycelia did not induce any significant changes in the positions on the PCA scores plot. This indicates that the simple addition of AZA did not perturb anything else in the system besides the inhibition of urate oxidase. This further supports the postulation that the small difference between *A. nidulans* wild-type spores in the presence of AZA and the *A. nidulans uaZ14* mutant spores is caused by residual Uox activity as opposed to a secondary inhibitory activity of AZA. Since AZA only inhibits urate oxidase in vivo, this observation would suggest a diminished likelihood of toxic side-effects arising from undesirable secondary activities by AZA. Of course, other mechanisms of drug toxicity, such as bioactive metabolites, may still be a concern.[83]

Conclusion

Using wild-type strains as metabolome references, the function of proteins and the in vivo activity of drugs can be monitored by combining NMR spectroscopy with principal component analysis. In effect, NMR metabolomic data provides in vivo information for the mechanism of action of potential drug candidates. The approach is equally applicable to therapeutic targets that utilize cell based systems, such as bacterial, cancer, endothelial, myocardial, renal, or tumor cell lines. Our results suggest that NMR metabolomics may provide an efficient approach to obtain preliminary in vivo data for chemical leads prior to initiating animal and clinical trials.

Acknowledgment. This work was supported by grants from the National Institutes of Health UNMC BRIN (P20 RR16469), Nebraska Tobacco Settlement Biomedical Research Development Funds and the Maude Hammond Fling Faculty Research Fellowship. Research was performed in facilities renovated with support from NIH (RR015468-01). We thank Prof. Miguel Penalva (CSIS, Madrid, Spain) for generously providing the *uaZ14* mutant.

Supporting Information Available: Chemical structure of metabolites discussed in the text, comparison of the PCA loadings and NMR spectra of *A. nidulans uaZ14* mutant and wild-type cells in the presence of AZA, NMR spectra comparing *A. nidulans pyrG89* mutant and wild-type cells, a diagram highlighting the intersection of the purine and pyrimidine biosynthetic pathways. This material is available free of charge via the Internet at http://pubs.acs.org.

References

(1) Zheng, C. J.; Han, L. Y.; Yap, C. W.; Xie, B.; Chen, Y. Z. Trends in exploration of therapeutic targets. *Drug News Perspect.* **2005**, *18* (2), 109−127.
(2) Ohlstein, E. H.; Johnson, A. G.; Elliott, J. D.; Romanic, A. M. New strategies in drug discovery. *Methods Mol. Biol.* **2005**, *316*, 1−11.
(3) Ahlborn, H.; Henderson, S.; Davies, N. No immediate pain relief for the pharmaceutical industry. *Curr. Opin. Drug Discov. Devel.* **2005**, *8* (3), 384−391.
(4) Dickson, M.; Gagnon, J. P. Key factors in the rising cost of new drug discovery and development. *Nat. Rev. Drug Discov.* **2004**, *3* (5), 417−429.
(5) Dickson, M.; Gagnon, J. P. The Cost of New Drug Discovery and Development. *Discovery Medicine* **2004**, *4* (22), 172−179.
(6) Booth, B.; Zemmel, R. Prospects for productivity. *Nat. Rev. Drug Discov.* **2004**, *3* (5), 451−456.
(7) Kola, I.; Landis, J. Opinion: Can the pharmaceutical industry reduce attrition rates? *Nat. Rev. Drug Discov.* **2004**, *3* (8), 711−716.
(8) Caldwell, G. W.; Ritchie, D. M.; Masucci, J. A.; Hageman, W.; Yan, Z. The new pre-preclinical paradigm: compound optimization in early and late phase drug discovery. *Curr. Topics Med. Chem.* **2001**, *1* (5), 353−366.
(9) Eddershaw, P. J.; Beresford, A. P.; Bayliss, M. K. ADME/PK as part of a rational approach to drug discovery. *Drug Discov. Today* **2000**, *5* (9), 409−414.
(10) Kubinyi, H.; Opinion: Drug research: myths, hype and reality. *Nat. Rev. Drug Discov.* **2003**, *2* (8), 665−668.
(11) Kennedy, T. Managing the drug discovery/development interface. *Drug Discov. Today* **1997**, *2*, 436−444.
(12) Sun, D.; Yu, L. X.; Hussain, M. A.; Wall, D. A.; Smith, R. L.; Amidon, G. L. In vitro testing of drug absorption for drug 'developability' assessment: Forming an interface between in vitro preclinical data and clinical outcome. *Curr. Opin. Drug Discov. Devel.* **2004**, *7* (1), 75−85.
(13) Hood, L.; Perlmutter, R. M. The impact of systems approaches on biological problems in drug discovery. *Nat. Biotechnol.* **2004**, *22* (10), 1215−1217.
(14) Berg, E. L.; Hytopoulos, E.; Plavec, I.; Kunkel, E. J. Approaches to the analysis of cell signaling networks and their application in drug discovery. *Curr. Opin. Drug Discov. Devel.* **2005**, *8* (1), 107−114.
(15) Weckwerth, W. Metabolomics in systems biology. *Ann. Rev. Plant Biol.* **2003**, *54*, 669−689.
(16) Kell, D. B. Metabolomics and systems biology: making sense of the soup. *Curr. Opin. Microbiol.* **2004**, *7* (3), 296−307.
(17) Goodacre, R.; Vaidyanathan, S.; Dunn, W. B.; Harrigan, G. G.; Kell, D. B. Metabolomics by numbers: acquiring and understanding global metabolite data. *Trends Biotechnol.* **2004**, *22* (5), 245−252.
(18) Fridman, E.; Pichersky, E. Metabolomics, genomics, proteomics, and the identification of enzymes and their substrates and products. *Curr. Opin. Plant Biol.* **2005**, *8* (3), 242−248.

(19) Zanders, E. D.; Gordon, R. D.; Gershater, C. J. L. The emergence of chemical genomics in drug discovery. *IDrugs* **2005**, *8* (11), 919−923.
(20) Nicholson Jeremy, K.; Connelly, J.; Lindon John, C.; Holmes, E. Metabonomics: a platform for studying drug toxicity and gene function. *Nat. Rev. Drug Discov.* **2002**, *1* (2), 153−161.
(21) Nicholson, J. K.; Lindon, J. C.; Holmes, E. "Metabonomics": understanding the metabolic responses of living systems to pathophysiological stimuli via multivariate statistical analysis of biological NMR spectroscopic data. *Xenobiotica* **1999**, *29* (11), 1181−1189.
(22) Wilson, I. D.; Plumb, R.; Granger, J.; Major, H.; Williams, R.; Lenz, E. M. HPLC−MS-based methods for the study of metabonomics. *J. Chromatogr. B: Anal. Technol. Biomed. Life Sci.* **2005**, *817* (1), 67−76.
(23) Halket, J. M.; Waterman, D.; Przyborowska, A. M.; Patel, R. K. P.; Fraser, P. D.; Bramley, P. M.; Chemical derivatization and mass spectral libraries in metabolic profiling by GC/MS and LC/MS/MS. *J. Exp. Botany* **2005**, *56* (410), 219−243.
(24) Shockcor, J. P.; Holmes, E. Metabonomic applications in toxicity screening and disease diagnosis. *Curr. Top. Med. Chem.* **2002**, *2* (1), 35−51.
(25) Robertson, D. G.; Reily, M. D.; Sigler, R. E.; Wells, D. F.; Paterson, D. A.; Braden, T. K. Metabonomics: evaluation of nuclear magnetic resonance (NMR) and pattern recognition technology for rapid in vivo screening of liver and kidney toxicants. *Toxicol. Sci.* **2000**, *57* (2), 326−337.
(26) Van der Greef, J.; Davidov, E.; Verheij, E.; Vogels, J.; Van der Heijden, R.; Adourian, A. S.; Oresic, M.; Marple, E. W.; Naylor, S. The role of metabolomics in systems biology: a new vision for drug discovery and development. *Metab. Profiling* **2003**, 171−198.
(27) Navon, G.; Burrows, H.; Cohen, J. S. Differences in metabolite levels upon differentiation of intact neuroblastoma * glioma cells observed by proton NMR spectroscopy. *FEBS Lett.* **1983**, *162* (2), 320−323.
(28) Pfeuffer, J.; Tkac, I.; Provencher, S. W.; Gruetter, R. Toward an in Vivo Neurochemical Profile: Quantification of 18 Metabolites in Short-Echo-Time 1H NMR Spectra of the Rat Brain. *J. Magn. Res.* **1999**, *141* (1), 104−120.
(29) Keun, H. C.; Ebbels, T. M. D.; Antti, H.; Bollard, M. E.; Beckonert, O.; Holmes, E.; Lindon, J. C.; Nicholson, J. K. Improved analysis of multivariate data by variable stability scaling: application to NMR-based metabolic profiling. *Anal. Chim. Acta* **2003**, *490* (1−2), 265−276.
(30) Lamers, R.-J. A. N.; DeGroot, J.; Spies-Faber, E. J.; Jellema, R. H.; Kraus, V. B.; Verzijl, N.; TeKoppele, J. M.; Spijksma, G. K.; Vogels, J. T. W. E.; van der Greef, J.; van Nesselrooij, J. H. J. Identification of disease- and nutrient-related metabolic fingerprints in osteoarthritic guinea pigs. *J. Nutrit.* **2003**, *133* (6), 1776−1780.
(31) Stoyanova, R.; Brown, T. R. NMR spectral quantitation by principal component analysis. *NMR Biomed.* **2001**, *14* (4), 271−277.
(32) Lindon, J. C.; Holmes, E.; Nicholson, J. K. Pattern recognition methods and applications in biomedical magnetic resonance. *Prog. Nucl. Magn. Reson. Spectrosc.* **2001**, *39* (1), 1−40.
(33) Griffin, J. L. The potential of metabonomics in drug safety and toxicology. *Drug Discov. Today: Technol.* **2004**, *1* (3), 285−293.
(34) Raamsdonk, L. M.; Teusink, B.; Broadhurst, D.; Zhang, N.; Hayes, A.; Walsh, M. C.; Berden, J. A.; Brindle, K. M.; Kell, D. B.; Rowland, J. J.; Westerhoff, H. V.; Van Dam, K.; Oliver, S. G. A functional genomics strategy that uses metabolome data to reveal the phenotype of silent mutations. *Nat. Biotechnol.* **2001**, *19* (1), 45−50.
(35) Bundy, J. G.; Willey, T. L.; Castell, R. S.; Ellar, D. J.; Brindle, K. M. Discrimination of pathogenic clinical isolates and laboratory strains of *Bacillus cereus* by NMR-based metabolomic profiling. *FEMS Microbiol. Lett.* **2005**, *242* (1), 127−136.
(36) Nielsen, K. F.; Smedsgaard, J.; Larsen, T. O.; Lund, F.; Thrane, U.; Frisvad, J. C. Chemical identification of fungi: metabolite profiling and metabolomics. *Mycol. Ser.* **2004**, *21*, 19−35.
(37) Casselton, L.; Zolan, M. The art and design of genetic screens: filamentous fungi. *Nat. Rev. Genet.* **2002**, *3* (9), 683−697.
(38) Girmenia, C.; Martino, P. New antifungal drugs and new clinical trials: interpreting results may be difficult. *Curr. Opin. Oncol.* **2003**, *15* (4), 283−288.
(39) Harris, S. D.; Morrell, J. L.; Hamer, J. E. Identification and characterization of Aspergillus nidulans mutants defective in cytokinesis. *Genetics* **1994**, *136* (2), 517−532.
(40) Bergmann, F.; Ungar-Waron, H.; Kwietny-Govrin, H. Action of 8-azaguanine and 8-azaxanthine on *Pseudomonas aeruginosa.* **1964**, *91*, (2), 270−276.
(41) Norris, E. R.; Roush, A. The competitive inhibition of uricase activity by 8-azaguanine and by 8-azaxanthine. *Arch. Biochem.* **1950**, *28*, 465−466.
(42) Oestreicher, N.; Sealy-Lewis, H. M.; Scazzocchio, C. Characterization, cloning and integrative properties of the gene encoding urate oxidase in Aspergillus nidulans. *Gene* **1993**, *132* (2), 185−192.
(43) Oakley, B. R.; Rinehart, J. E.; Mitchell, B. L.; Oakley, C. E.; Carmona, C.; Gray, G. L.; May, G. S. Cloning, mapping and molecular analysis of the pyrG (orotidine-5′-phosphate decarboxylase) gene of *Aspergillus nidulans*. *Gene* **1987**, *61* (3), 385−399.
(44) Halouska, S.; Powers, R. Negative impact of noise on the principal component analysis of NMR data. *J. Magn. Reson.* **2006**, *178* (1), 88−95.
(45) Dijkema, C.; Kester, H. C.; Visser, J. 13C NMR studies of carbon metabolism in the hyphal fungus Aspergillus nidulans. *Proc. Nat'l. Acad. Sci., U.S.A.* **1985**, *82* (1), 14−8.
(46) Hofmann, G.; McIntyre, M.; Nielsen, J. Fungal genomics beyond *Saccharomyces cerevisiae*? *Curr. Opin. Biotechnol.* **2003**, *14* (2), 226−231.
(47) Smedsgaard, J.; Nielsen, J. Metabolite profiling of fungi and yeast: from phenotype to metabolome by MS and informatics. *J. Exp. Botany* **2005**, *56* (410), 273−286.
(48) Sims Andrew, H.; Gent Manda, E.; Robson Geoffrey, D.; Dunn-Coleman Nigel, S.; Oliver Stephen, G. Combining transcriptome data with genomic and cDNA sequence alignments to make confident functional assignments for Aspergillus nidulans genes. *Mycol. Res.* **2004**, *108* (Pt 8), 853−857.
(49) McCluskey, K. The Fungal Genetics Stock Center: from molds to molecules. *Adv. Appl. Microbiol.* **2003**, *52*, 245−262.
(50) Sealy-Lewis, H. M.; Scazzocchio, C.; Lee, S. A mutation defective in the xanthine alternative pathway of Aspergillus nidulans. Its use to investigate the specificity of uaY mediated induction. *Mol. General Genet.* **1978**, *164* (3), 303−308.
(51) Scazzocchio, C.; Darlington, A. J. Induction and repression of the enzymes of purine breakdown in *Aspergillus nidulans*. *Biochim. Biophys. Acta, Nucl. Acids Protein Synth.* **1968**, *166* (2), 557−568.
(52) Scazzocchio, C. The purine degradation pathway, genetics, biochemistry and regulation. *Prog. Ind. Microbiol.* **1994**, *29*, 221−257.
(53) Oestreicher, N.; Scazzocchio, C. Sequence, regulation, and mutational analysis of the gene encoding urate oxidase in Aspergillus nidulans. *J. Biol. Chem.* **1993**, *268* (31), 23382−23389.
(54) Retailleau, P.; Colloc'h, N.; Vivares, D.; Bonnete, F.; Castro, B.; El Hajji, M.; Mornon, J. P.; Monard, G.; Prange, T. Complexed and ligand-free high-resolution structures of urate oxidase (Uox) from Aspergillus flavus: a reassignment of the active-site binding mode. *Acta Crystallogr., Section D: Biol. Crystallogr.* **2004**, *D60* (3), 453−462.
(55) Colloc'h, N.; El Hajji, M.; Bachet, B.; L'Hermite, G.; Schiltz, M.; Prange, T.; Castro, B.; Mornon, J.-P. Crystal structure of the protein drug urate oxidase-inhibitor complex at 2.05.ANG. resolution. *Nat. Struct. Biol.* **1997**, *4* (11), 947−952.
(56) Miller, B. G.; Insight into the catalytic mechanism of orotidine 5′-phosphate decarboxylase from crystallography and mutagenesis. *Top. Curr. Chem.* **2004**, *238*, 43−62.
(57) Radzicka, A.; Wolfenden, R. A proficient enzyme. *Science* **1995**, *267*, (5194), 90−93.
(58) Nara, T.; Hshimoto, T.; Aoki, T. Evolutionary implications of the mosaic pyrimidine-biosynthetic pathway in eukaryotes. *Gene* **2000**, *257* (2), 209−222.
(59) Yamada, K.; Morisaki, M.; Kumaoka, H. Different biosynthetic pathways of the pyrimidine moiety of thiamin in prokaryotes and eukaryotes. *Biochim. Biophys. Acta, Gen. Subjects* **1983**, *756* (1), 41−48.
(60) Wu, N.; Pai, E. F. Crystallographic studies of native and mutant orotidine 5′-phosphate decarboxylases. *Top. Curr. Chem.* **2004**, *238*, 23−42.
(61) Sigoillot, F. D.; Berkowski, J. A.; Sigoillot, S. M.; Kotsis, D. H.; Guy, H. I. Cell Cycle-dependent Regulation of Pyrimidine Biosynthesis. *J. Biol. Chem.* **2003**, *278* (5), 3403−3409.
(62) West, T. P. Regulation of pyrimidine nucleotide formation in *Pseudomonas reptilivora*. *Lett. Appl. Microbiol.* **2004**, *38* (2), 81−86.
(63) West, T. P. Control of pyrimidine biosynthesis in "Pseudomonas alkanolytica" ATCC 21034. *J. Basic Microbiol.* **2004**, *44* (3), 253−257.

(64) West, T. P. Regulation of pyrimidine nucleotide formation in Pseudomonas taetrolens ATCC 4683. *Microbiol. Res.* **2004**, *159* (1), 29−33.
(65) Geigenberger, P.; Regierer, B.; Nunes-Nesi, A.; Leisse, A.; Urbanczyk-Wochniak, E.; Springer, F.; van Dongen, J. T.; Kossmann, J.; Fernie, A. R. Inhibition of de novo pyrimidine synthesis in growing potato tubers leads to a compensatory stimulation of the pyrimidine salvage pathway and a subsequent increase in biosynthetic performance. *Plant Cell* **2005**, *17* (7), 2077−2088.
(66) Hata, H.; Niimura, M.; Yano, A. Effects of nucleic acid inhibitors on the development of *Angiostrongylus costaricensis* in vitro. *J. Vet. Med. Sci.* **1998**, *60* (10), 1153−1155.
(67) Ahluwalia, G. S.; Gao, W.-Y.; Mitsuya, H.; Johns, D. G. 2′, 3′-Didehydro-3′-deoxythymidine: regulation of its metabolic activation by modulators of thymidine-5′-triphosphate biosynthesis. *Mol. Pharmacol.* **1996**, *50* (1), 160−165.
(68) Singhal, R. L.; Yeh, Y. A.; Sledge, G. W., Jr.; Weber, G. Elevated deoxycytidine and thymidine kinase activities in human breast carcinoma cells: Inhibition by difluorodeoxycytidine and azidodeoxythymidine. *Proceedings of the International Cancer Congress, Free Papers and Posters,* 16th, New Delhi **1994**, 2, 1377−1381.
(69) Smith, D. A.; Jones, B.; Variability in drug response as a factor in drug design. *Curr. Opin. Drug Discov. Devel.* **1999**, *2* (1), 33−41.
(70) Recanatini, M.; Bottegoni, G.; Cavalli, A.; In silico antitarget screening. *Drug Discov. Today: Technol.* **2004**, *1* (3), 209−215.
(71) Coughlan, C. M.; Brodsky, J. L. Use of yeast as a model system to investigate protein conformational diseases. *Mol. Biotechnol.* **2005**, *30* (2), 171−180.
(72) Golovina, T. N.; Morrison, S. E.; Eisenlohr, L. C.; The Impact of Misfolding versus Targeted Degradation on the Efficiency of the MHC Class I−Restricted Antigen Processing. *J. Immunol.* **2005**, *174* (5), 2763−2769.
(73) Lelouard, H.; Ferrand, V.; Marguet, D.; Bania, J.; Camosseto, V.; David, A.; Gatti, E.; Pierre, P. Dendritic cell aggresome-like induced structures are dedicated areas for ubiquitination and storage of newly synthesized defective proteins. *J. Cell Biol.* **2004**, *164* (5), 667−675.
(74) Schubert, U.; Anton, L. C.; Gibbs, J.; Norbury, C. C.; Yewdell, J. W.; Bennink, J. R. Rapid degradation of a large fraction of newly synthesized proteins by proteasomes. *Nature (London)* **2000**, *404* (6779), 770−774.
(75) Maglott, D. R.; Nierman, W. C. Clone and genomic repositories at the American Type Culture Collection. *Genomics* **1990**, *8* (3), 601−605.
(76) Mannhaupt, G.; Montrone, C.; Haase, D.; Mewes, H. W.; Aign, V.; Hoheisel Jorg, D.; Fartmann, B.; Nyakatura, G.; Kempken, F.; Maier, J.; Schulte, U. What is in the genome of a filamentous fungus? Analysis of the Neurospora genome sequence. *Nucleic Acids Res.* **2003**, *31* (7), 1944−1954.
(77) Bosher, J. M.; Labouesse, M.; RNA interference: genetic wand and genetic watchdog. *Nat. Cell Biol.* **2000**, *2* (2), E31−E36.
(78) Zamore, P. D. RNA interference: listening to the sound of silence. *Nat. Struct. Biol.* **2001**, *8* (9), 746−750.
(79) Qiao, Y.; Molina, H.; Pandey, A.; Zhang, J.; Cole, P. A. Chemical Rescue of a Mutant Enzyme in Living Cells. *Science* **2006**, *311* (5765), 1293−1297.
(80) Wise, E. L.; Yew, W. S.; Akana, J.; Gerlt, J. A.; Rayment, I. Evolution of Enzymatic Activities in the Orotidine 5′-Monophosphate Decarboxylase Suprafamily: Structural Basis for Catalytic Promiscuity in Wild-Type and Designed Mutants of 3-Keto-L-gulonate 6-Phosphate Decarboxylase. *Biochemistry* **2005**, *44* (6), 1816−1823.
(81) Dynesen, J.; Nielsen, J. Branching is coordinated with mitosis in growing hyphae of *Aspergillus nidulans*. *Fungal Genet. Biol.* **2003**, *40* (1), 15−24.
(82) Timberlake, W. E. Molecular genetics of *Aspergillus* development. *Ann. Rev. Genet.* **1990**, *24*, 5−36.
(83) Zhou, S.; Chan, E.; Duan, W.; Huang, M.; Chen, Y.-Z. Drug bioactivation, covalent binding to target proteins and toxicity relevance. *Drug Metabol. Rev.* **2005**, *37* (1), 41−213.

PR060114V